

Am Chem Soc. Author manuscript; available in PMC 2013 September 13.

Published in final edited form as:

J Am Chem Soc. 2008 June 25; 130(25): 8038–8043. doi:10.1021/ja801412b.

Selective Detection of Mercury (II) Ion Using Nonlinear Optical Properties of Gold Nanoparticles

Gopala Krishna Darbha, Anant Kumar Singh, Uma Shanker Rai, Eugene Yu, Hongtao Yu, and Paresh Chandra Ray

Department of Chemistry, Jackson State University, Jackson, Mississippi 39217

Paresh Chandra Ray: paresh.c.ray@jsums.edu

Abstract

Contamination of the environment with heavy metal ions has been an important concern throughout the world for decades. Driven by the need to detect trace amounts of mercury in environmental samples, this article demonstrates for the first time that nonlinear optical (NLO) properties of MPA–HCys–PDCA-modified gold nanoparticles can be used for rapid, easy and reliable screening of Hg(II) ions in aqueous solution, with high sensitivity (5 ppb) and selectivity over competing analytes. The hyper Rayleigh scattering (HRS) intensity increases 10 times after the addition of 20 ppm $\mathrm{Hg^{2+}}$ ions to modified gold nanoparticle solution. The mechanism for HRS intensity change has been discussed in detail using particle size-dependent NLO properties as well as a two-state model. Our results show that the HRS assay for monitoring $\mathrm{Hg(II)}$ ions using MPA–HCys–PDCA-modified gold nanoparticles has excellent selectivity over alkali, alkaline earth ($\mathrm{Li^+}$, $\mathrm{Na^+}$, $\mathrm{K^+}$, $\mathrm{Mg^{2+}}$, $\mathrm{Ca^{2+}}$), and transition heavy metal ions ($\mathrm{Pb^{2+}}$, $\mathrm{Pb^+}$, $\mathrm{Mn^{2+}}$, $\mathrm{Fe^{2+}}$, $\mathrm{Cu^{2+}}$, $\mathrm{Ni^{2+}}$, $\mathrm{Zn^{2+}}$, $\mathrm{Cd^{2+}}$).

Introduction

Contamination of the environment with heavy metal ions has been an important concern throughout the world for decades. Mercury is one of the most toxic elements on the planet, probably second only to plutonium. Mercury is a known environmental pollutant routinely released from coal-burning power plants, oceanic and volcanic emissions, gold mining, and solid waste incineration. The long atmospheric residence time of Hg⁰ vapor and its oxidation to soluble inorganic Hg(II) provides a pathway for contaminating vast amounts of water and soil. Bacteria living in the sediments of aqueous environments transform inorganic Hg(II) into methylmercury, a potent neurotoxin that concentrates through the food chain in the tissues of fish and marine mammals. Since with sufficient exposure all mercurybased toxins damage the central nervous system and other organs or organ systems such as the liver or gastrointestinal tract, it is important to develop highly sensitive and selective Hg sensor that can provide real-time determination of Hg levels in the environment, water, and food. A number of fluorescence-based probes and sensors for detection of Hg(II) have been reported.²⁻¹⁰ However, many fluorescent small-molecule-based Hg(II) sensors presented to date are quenched upon Hg(II) coordination, often rely on an irreversible Hg(II)-dependent chemical reaction to give fluorescence turn-on, and/or require organic solvent systems. Most of these sensors display drawbacks in terms of actual applicability such as the lack of water solubility, cross-sensitivity toward other metal ions, weak fluorescence enhancement factor, and short emission wavelengths. Thus, the development of facile and practical assays for

Hg(II) remains a challenge. In the last two years our group ¹¹ and others ^{12–15} have directed their attention to gold nanoparticle-based colorimetric and nanomaterial based surface energy transfer (NSET) assay on recognition and detection of mercury ions in aqueous solution. But these assays identify mercury after the nanoparticle has been modified with a covalently linked DNA or labeled with a fluorescent tag. The necessity of tagging makes it costly to use those techniques as sensors for real life. Driven by the need, we demonstrate in this article, for the first time, that second-order nonlinear optical (NLO) properties of gold nanoparticles can be used for screening mercury from environmental samples without any DNA or fluorescent tag, with excellent sensitivity (5 ppb) and selectivity.

NLO properties have been monitored using a hyper-Rayleigh scattering (HRS) technique. The HRS technique 16-26 is based on light scattering. The HRS or nonlinear light scattering can be observed from fluctuations in symmetry, caused by rotational fluctuations. This is a second harmonic generation experiment in which the light is scattered in all directions rather than as a narrow coherent beam. The technique can be easily applied to study a very wide range of materials because electrostatic fields and phase matching are not required. Other advantages are that the polarization analysis gives information about the tensor properties, and spectral analysis of the scattered light gives information about the dynamics. Recently 19,20 we have shown that the HRS technique can be used to achieve detection of pathogenic DNA with excellent sensitivity (100 pM) and selectivity (single base-pair mismatch) through NLO properties of gold nanoparticle. Hupp and co-workers ¹⁷ have reported a concept on gold nanoparticle-based HRS and colorimetric techniques for the detection of small concentrations of aqueous heavy metal ions, including toxic metals such as lead, cadmium, and mercury. Their data (Figures 1, 2, and 3 in reference 17) show the colorimetric, TEM, and HRS intensity change due to the addition of Pb²⁺ ion. Although they have not presented any data for Hg²⁺ ion, they have indicated that similar responses were obtained with Hg²⁺- and Cd²⁺-containing solutions. Due to the lack of selectivity, the gold nanoparticle-based HRS assay reported by Kim et al. ¹⁷ cannot be applied to detect heavy metal ions from environmental samples. Here we report a highly selective and sensitive HRS assay for mercury (II) recognition at 5 ppb level in aqueous solution using gold nanoparticles modified with mercaptopropionic acid (MPA), homocystine (HCys), and 2,6pyridinedicarboxylic acid (PDCA). Our results show that the HRS assay for monitoring Hg(II) ions using MPA-Cys-PDCA-modified gold nanoparticles have excellent selectivity over alkali, alkaline earth (Li⁺, Na⁺, K⁺, Mg²⁺, Ca²⁺) and transition heavy metal ions (Pb²⁺, Pb⁺, Mn²⁺, Fe²⁺, Cu²⁺, Ni²⁺, Zn²⁺, Cd²⁺).

Experimental Section

Hydrogen tetrachloroaurate (HAuCl₄·3H₂O), NaBH₄, mercaptopropionic acid (MPA), homocystine (HCys), 2,6-pyridinedicarboxylic acid, buffer solution, sodium chloride, and sodium citrate were purchased from Sigma-Aldrich and used without further purification.

Gold Nanoparticle Synthesis

Gold nanoparticles of diameters of 15 nm or more were synthesized using the reported method. 11,19,20 Gold nanoparticles of different sizes and shapes were synthesized by controlling the ratio of the HAuCl₄·3H₂O, and sodium citrate concentrations as we reported recently. 11,19,20,27,28 For smaller gold nanoparticles, we have used the sodium borohydride method as reported before. To 18 mL of deionized H₂O were added 0.5 mL of 0.01 M HAuCl₄ trihydrate in water and 0.5 mL of 0.01 M sodium citrate in water and stirred. Next, 0.5 mL of freshly prepared 0.1 M NaBH₄ was added, and the solution color changed from colorless to orange. Stirring was stopped, and the solution was left undisturbed for 2 h. The resulting spherical gold nanoparticles were 4 nm in diameter. Transmission electron microscope (TEM) and UV–visible absorption spectrum were used to characterize the

nanoparticles. The particle concentration was measured by UV–visible spectroscopy using the molar extinction coefficients at the wavelength of the maximum absorption of each gold colloid as reported recently $^{11,25-28}$ [$_{(15)}$ $_{528nm}$ = 3.6×10^{8} cm $^{-1}$ M $^{-1}$, $_{(30)}$ $_{530nm}$ = 3.0×10^{9} cm $^{-1}$ M $^{-1}$, $_{(40)}$ $_{533nm}$ = 6.7×10^{9} cm $^{-1}$ M $^{-1}$, $_{(50)}$ $_{535nm}$ = 1.5×10^{10} cm $^{-1}$ M $^{-1}$, $_{(60)}$ $_{540nm}$ = 2.9×10^{10} cm $^{-1}$ M $^{-1}$, and $_{(80)}$ $_{550nm}$ = 6.9×10^{10} cm $^{-1}$ M $^{-1}$].

Gold Nanoparticle Surface Modification

To detect Hg(II) ion selectively, we modified the surface of the gold nanoparticle with mercaptopropionic acid (MPA) and homocystine (bound to the gold nanoparticle surface through a Au–S bond), and we added a chelating ligand PDCA, to the solution, as we discussed before. The gold nanoparticle surface was attached with MPA and HCys through a –SH bond using a method similar to one we have described before. We have added 10 mM MPA (10 μ L) and 2 mM HCys (10 μ L) to the gold nanoparticle solution (15 nM, 10 mL) with stirring. After 2 h, (5–8) mM NaBH₄ was added, and the mixture was left for few hours without disturbance.

For the HRS experiments we have used a mode-locked Ti: sapphire laser delivering at fundamental wavelengths of 860 nm with a pulse duration of about 150 fs at a repetition rate of 80 MHz. After passing through a low-pass filter, a fundamental beam of about 100 mW was focused into a quartz cell containing the aqueous solutions of the metallic particles. The HRS light was separated from its linear counterpart by a high-pass filter and a monochromator and then was detected with a cooled photomultiplier tube; the pulses were then counted with a photon counter. The fundamental input beam was linearly polarized, and the input angle of polarization was selected with a rotating half-wave plate. In all experiments reported, the polarization state of the harmonic light was vertically polarized.

Results and Discussion

The intensity $I_{\rm HRS}$ of the hyper-Rayleigh signal from an aqueous solution of gold nanoparticles can be expressed as $^{16-25}$

$$I_{\rm HRS} = G \left\langle N_w \beta_w^2 + N_{\rm nano} \beta_{\rm nano}^2 \right\rangle I_\omega^2 e^{-N} {\rm nano}^{\varepsilon_{2\omega} 1}$$
 (1)

where G is a geometric factor, $N_{\rm w}$ and $N_{\rm nano}$ the number of water molecules and gold nanoparticles per unit volume, and nano are the quadratic hyperpolarizabilities of a single water molecule and a single gold nanoparticle, 2 is the molar extinction coefficient of the gold nanoparticle at 2, 1 is the path length and I the fundamental intensity. The exponential factor accounts for the losses through absorption at the harmonic frequency. The HRS signal intensities were normalized to the square of the incident light intensity. To understand whether the two-photon scattering intensity at 430 nm light is due to second harmonic generation, we performed a power-dependent as well as a concentration-dependent study. Figure 1 shows the output signal intensities at 430 nm from MPA-HCys-PDCAmodified gold nanoparticles at different powers of 860 nm incident light. A linear nature of the plot implies that the doubled light is indeed due to the HRS signal. To extract absolute values for the hyperpolarizabilities, the normalized intensities were normalized again with paranitro aniline (p-NA) in methanol. The measured hyperpolarizability for p-NA was 34.6 \times 10⁻³⁰ esu at 1064 nm excitation, which is in complete agreement with the literature values. ¹⁶ By using $_{\rm w} = 0.56 \times 10^{-30}$ esu, as reported in the literature, we found out $_{\rm nano} =$ 78×10^{-26} esu for 50 nm gold nanoparticle and 80.5×10^{-26} esu for MPA-and PDCAmodified gold nanoparticle. Our measured value for 50 nm gold nanoparticles matches very well with the reported values by other groups. 25,26

The optical responses of particles that are small compared to the wavelength can be described usually in the framework of electric-dipole approximation. However, when the particle size approaches the wavelength, the dipolar picture may no longer provide a complete description, and higher multipolar interactions should be considered, as we discussed before.²⁰ Since there is a center of inversion in nanoparticle, the HRS intensity arising from a gold nanoparticle cannot be due to electric-dipole contribution. At the microscopic scale, the breaking of the centrosymmetry is required for the harmonic generation process at the surface of the particle. Considering the size of a nanoparticle (above 50 nm), the approximation that assumes that the electromagnetic fields are spatially constant over the volume of the particle is not suitable anymore. As a result, the total nonlinear polarization consists of different contributions such as multipolar radiation of the harmonic energy of the excited dipole and possibly of higher multipoles, as we discussed in our previous publication or reported by others. ^{20,24–26} The HRS intensity therefore also consists of several contributions. The first one is the electric dipole approximation, which may arise due to the defects in nanoparticle. This contribution is actually identical to the one observed for any noncentrosymmetrical pointlike objects such as efficient rodlike push-pull molecules. The second contribution is a multipolar contribution such as an electric quadrupole contribution. This contribution is very important when the size of the particle is no longer negligible when compared to the wavelength, as we reported before. ^{20,24–26}

Figure 2 shows how the HRS intensity varies after addition of different concentrations of Hg (II) into modified gold nanoparticle solution (12 nM). We observed a very distinct HRS intensity change (about 1.2 times) even after addition of 5 ppb Hg(II) as shown in Figure 2b.

To evaluate the sensitivity of our HRS technique, different concentrations of Hg(II) from one stock solution were evaluated. As shown in Figure 2a, the HRS intensity is highly sensitive to the concentration of Hg(II) ions and after the concentration of 40 ppm Hg(II) ions, the HRS intensity remains unchanged. Linear correlation was found between the HRS intensity and concentration of Hg(II) ions over the range of 5–100 ppb (as shown in Figure 2b) and 1–10 ppm (as shown in Figure 2c). The environmental protection agency (EPA) standard for the maximum allowable level of Hg(II) in drinking water is 2 ppb, ¹ which is about same order of magnitude as our HRS assay sensitivity.

We also noted that when the HRS intensity changes about 9 times at the concentration of 10 ppm mercury ion, the visible color changes (as shown in Figure 3b) can be observed. Thus, the color change can only be observed after the addition of 10 ppm of mercury ions, whereas HRS changes (1.2 times) can be observed even at the concentration of 5 ppb, which indicates that our HRS assay is about 3 orders of magnitude more sensitive that the usual colorimetric technique.

To understand the HRS intensity changes with the addition of different concentrations of Hg ions, we have also performed absorption and TEM studies before and after addition of mercury ions of different concentrations. We noted the shift in the plasmon band energy to longer wavelength (about 150–200 nm, as shown in Figure 3) after the addition of Hg(II) ions in MAP–gold-nanoparticle–PDCA solution, which indicated strong aggregation of gold nanoparticles (as shown in Figure 4). Figure 4 shows the TEM images of gold nanoparticle–MPA–PDCA solution in the presence and absence of Hg (II) ions. Aggregation in the presence of Hg (II) ions is due to binding with chelating ligands, yielding both a substantial shift in the plasmon band energy to longer wavelength and a red-to-blue color change. After the addition of mercury, the HRS intensity change can be due to several factors and these are as follows: (1) Since after mercury addition, aggregation takes place, gold nanoparticle looses the center of symmetry and as a result, one can expect significant amount of electric dipole contribution to the HRS intensity. Since electric dipole contributes several times

higher than that of multipolar moments, we expect the HRS intensity to increase with aggregation. (2) Since absorption maximum changes from 520 to 720 nm due to the aggregation, a two-level model that has been extensively used for donor–acceptor NLO chromophores can be used to explain the difference of first-order nonlinearity due to the change in color of gold nanoparticles. According to the two-state model, ²⁹

$$\beta^{\text{two state}} = \frac{3\mu_{\text{eg}}^2 \Delta \mu_{\text{eg}}}{E_{\text{eg}}^2} \frac{\omega_{\text{eg}}^2}{(1 - 4\omega^2 / \omega_{\text{eg}}^2)(\omega_{\text{eg}}^2 - \omega^2)}$$
(2)
$$\text{dispersion factor}$$

where μ_{eg} is the transition dipole moment between the ground state $||g\rangle$ and the charge-transfer excited state $||e\rangle$, μ_{eg} is the difference in dipole moment and E_{10} is the transition energy. As the color changes, the $_{max}$ changes from 520 to 720 nm, should change tremendously and as a result HRS intensity changes. (3) Since size increases tremendously with aggregation, the HRS intensity should increase with the increase in particle size.

To detect Hg(II) ion selectively, we modified the surface of the gold nanoparticle with MPA and HCys (bound to the gold nanoparticle surface through the Au-S bond), and we added a chelating ligand PDCA to the solution as we discussed before. When we modified the surface with only MPA or HCys (bound to the gold nanoparticle surface through the Au-S bond), our assay shows negligible responses toward Fe(II), Mn(II), Zn(II), Ni(II), K (II), Cr(III), and Sr(II), but we have noted substantial shift in the plasmon band energy to longer wavelengths and a red-to-blue color change, in the presence of Hg(II), Pb(II) as well as Cd(II). It has been reported³⁰ in the literature that the stability constants between heavy metal ions and chelating ligand like MPA are $\log K(Pb) = 4.1$, $\log K(Hg) = 10.1$, $\log K(Cd)$ = 3.2, and log K(Zn) = 1.8 respectively. So stability constant of mercury–MPA complex is about 6 orders of magnitudes higher than with other interfering metal ions. But when we modified the surface with both MPA and HCys, (5:1) our assays shows negligible responses toward Cd(II), but we noted red-to-blue color change, in the presence of Hg(II) or Pb(II). Further higher selectivity of our probe toward Hg(II) ions was achieved by adding another chelating ligand, PDCA. Stability constants of heavy metal ions with PDCA are $\log K(Pb) =$ 8.2, $\log K(\text{Hg}) = 20.2$, $\log K(\text{Cd}) = 10.0$, and $\log K(\text{Mn}) = 8.5$. So PDCA will be able to form much more stable complex with Hg (II) than with other metal ions. Therefore, when we modified the surface of the gold nanoparticle with MPA and HCys and we added a chelating ligand PDCA, to the solution, excellent selectivity was achieved over alkali, alkaline earth, and transition heavy metal ions. To achieve better selectivity, we added PDCA to each MPA-HCys-gold nanoparticle solution at a concentration about 7–10 times greater than that of Hg(II) ions. Figure 5a shows the colorimetric response, and Figure 5b shows the HRS response in the presence of various environmentally relevant metal ions. Our result shows excellent selectivity over alkali, alkaline earth (Li⁺, Na⁺, K⁺, Mg²⁺, Ca²⁺) and transition heavy metal ions (Pb²⁺, Pb⁺, Mn²⁺, Fe²⁺, Cu²⁺, Ni²⁺, Zn²⁺, Cd²⁺). We also tested the selectivity in the presence of only PDCA, our results show red-to-blue color change, in the presence of Hg(II), Fe(II) and Cr(III). From all the results we conclude that modification of the gold nanoparticle surface with MPA and HCys is very important for increasing the selectivity toward Hg(II). We believe that PDCA ligands bound to the MPA-HCys-AuNP species through Au-N bonds improved the selectivity toward Hg(II) ions through a cooperative effect, while the PDCA ligands in the bulk solutions formed complexes with other metal ions, suppressing their interference with the probes.

To understand the response rate of the HRS signal upon addition of $Hg(\Pi)$ we have measured the HRS intensity at different time intervals, and our HRS experimental data indicate that the reaction is complete within 400~s.

Conclusions

In conclusion, in this article, we have demonstrated for the first time a label-free, selective, and highly sensitive HRS assay for mercury (II) recognition in 5 ppb level in aqueous solution. Our HRS assay will have several advantages, and these are: (i) one does not need to use DNA or fluorescenet dyes to probe mercury (II) ion in solution by the HRS technique; (ii) it can be 2–3 orders of magnitude more sensitive than the usual colorimetric technique; (iii) it is highly selective; and (iv) it takes only 6–7 min to find out the concentration of mercury in aqueous solution. Our experimental results reported here open up a new possibility of rapid, easy, and reliable diagnosis of toxic metal ions from environmental samples by measuring the HRS intensity of MPA–HCys–PDCA-modified gold nanoparticles. For developing a practical assay, more research needs to be done on improvement of the HRS experimental system, and the HRS intensity variation with the shape and size of metal nanoparticles should be investigated. It may be possible to improve the HRS intensity by several orders of magnitudes by choosing proper materials and detection systems. We believe that the HRS method has enormous potential for application of toxic metal detection from environmental samples.

Acknowledgments

P.C.R. thanks NSF-PREM Grant DMR-0611539 and NSF-MRI Grant 0421406 for their generous funding. We thank Sara H. Bayley, Instrumentation Facilities Coordinator, University of Southern Mississippi for helping to acquire TEM data. We also thank reviewers whose valuable suggestions improved the quality of the manuscript.

References

- 1. http://www.epa.gov
- 2. Harano K, Hiraoka S, Shionoya M. J Am Chem Soc. 2007; 129:5300. [PubMed: 17411034]
- 3. Butler OT, Cook JM, Harrington CF, Hill SJ, Rieuwerts J, Miles DLJ. Anal Atom Spectrom. 2006; 21:217
- 4. Leermakers M, Baeyens W, Quevauviller P, Horvat M. Trends Anal Chem. 2005; 24:383.
- 5. Valeur, B., editor. Molecular Fluorescence: Principles and Applications. Wiley-VCH; Weinheim: 2002.
- Komatsu H, Miki T, Citterio D, Kubota T, Shindo Y, Kitamura Y, Oka K, Suzuki K. J Am Chem Soc. 2005; 127:10798. [PubMed: 16076163]
- 7. Zhu XJ, Fu ST, Wong WK, Guo JP, Wong WYA. Angew Chem, Int Ed. 2005; 45:3150.
- 8. Mello JV, Finney NSA. J Am Chem Soc. 2005; 127:10124. [PubMed: 16028896]
- 9. Nolan EM, Lippard SJ. J Am Chem Soc. 2003; 125:14270. [PubMed: 14624563]
- 10. Caballero A, Martínez R, Lioveras V, Tatera I, Vidal-Gancedo J, Wurst K, Tárraga A, Molina P, Veciana J. J Am Chem Soc. 2005; 127:15666. [PubMed: 16277484]
- 11. Darbha GK, Ray A, Ray PC. ACS Nano. 2007; 1:208. [PubMed: 19206651]
- 12. Lee JS, Han MS, Mirkin CA. Angew Chem, Int Ed. 2007; 46:4093.
- 13. Huang CC, Chang HT. Anal Chem. 2006; 78:8332. [PubMed: 17165824]
- 14. Chih-Ching H, Zusing Y, Kun-Hong L, Huan-Tsung C. Angew Chem, Int Ed. 2007; 47:5549.
- 15. Xuejia X, Wang F, Xiaogang L. J Am Chem Soc. 2008; 130:3244. [PubMed: 18293973]
- 16. Clays K, Persoons A. Phys Rev Lett. 1991; 66:2980. [PubMed: 10043668]
- 17. Kim Y, Johnson RC, Hupp JT. Nano Lett. 2001; 1:165.
- 18. Viau L, Bidault S, Maury O, Brasselet S, Ledoux I, Zyss J, Ishow E, Nakatani K, Le Bozec H. J Am Chem Soc. 2004; 126:8386. [PubMed: 15237989]
- 19. Ray PC. Angew Chem, Int Ed. 2006; 45:1151.
- 20. Darbha GK, Rai US, Singh AK, Ray PC. Chem Eur J. 2008; 14:3896. [PubMed: 18348156]

21. Kang H, Evmenenko G, Dutta P, Clays K, Song K, Marks TJ. J Am Chem Soc. 2006; 128:6194.1. [PubMed: 16669690]

- 22. Coe BJ, Harries JL, Helliwell M, Jones LA, Asselberghs I, Clays K, Brunschwig BS, Harris JA, Garin J, Orduna J. J Am Chem Soc. 2006; 128:12192. [PubMed: 16967970]
- 23. Ghosh S, Krishnan A, Das PK, Ramakrishnan S. J Am Chem Soc. 2003; 125:1602. [PubMed: 12568621]
- 24. Chandra M, Indi SS, Das PK. J Phys Chem C. 2007; 111:10652.
- 25. Russier-Antoine I, Benichou E, Bachelier G, Jonin C, Brevet PF. J Phys Chem C. 2007; 111:9044.
- 26. Nappa JI, Russier-Antoine E, Benichou G, Bachelier C, Brevet PF. J Chem Phys. 2006; 125:184712. [PubMed: 17115784]
- 27. Ray PC, Fortner A, Darbha GK. J Phys Chem B. 2006; 110:20745. [PubMed: 17048879]
- 28. Kim CK, Kalluru RR, Singh JP, Fortner A, Griffin J, Darbha GK, Ray PC. Nanotechnology. 2006; 17:3085.
- 29. Oudar JL. J Chem Phys. 1977; 67:44.
- 30. Morel, FMM. Principles of Aquatic Chemistry. Wiley-Interscience; New York: 1983. p. 237
- 31. Norkus E, Stalnioniene I, Crans DC. Heteroat Chem. 2003; 14:625.

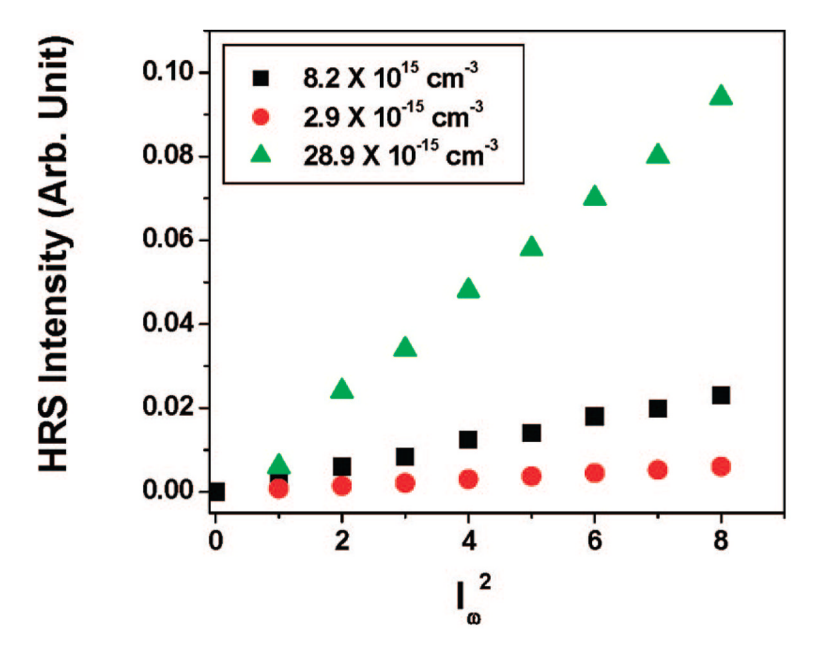


Figure 1. Power dependence of HRS intensity for different concentrations of gold nanoparticles.

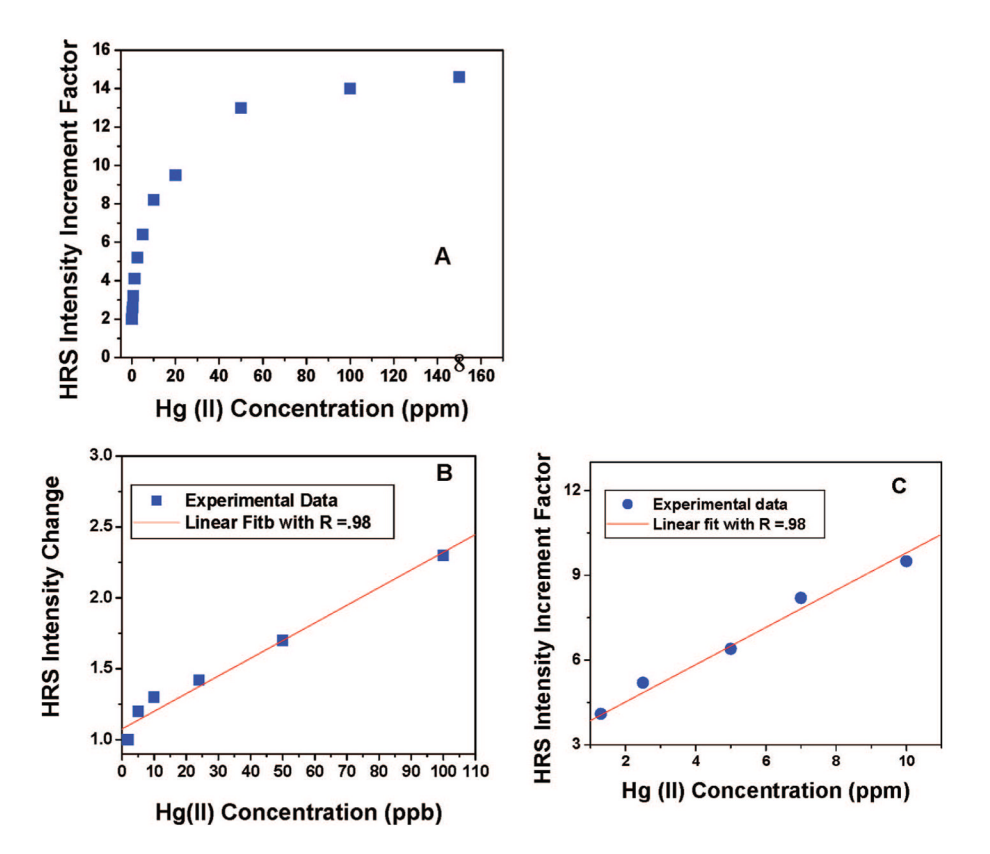


Figure 2.

(a) Plot of HRS intensity increment factor (ratio of the HRS intensity after the addition of Hg(II) to the HRS intensity before the addition of Hg(II) vs Hg(II) concentration in ppm.

(b) Plot of HRS intensity increment factor vs Hg(II) concentration in ppb. Linear correlation exists over the range of 5–100 ppb with R = 0.988. (c) Plot of HRS intensity increment factor vs Hg(II) concentration in ppb. Linear correlation exists over the range of 1–10 ppm with R = 0.988.

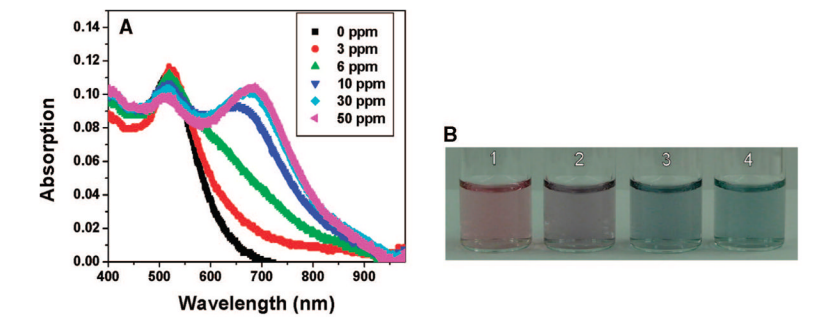


Figure 3.(a) Absorption profile of modified gold nanoparticles before and after addition of different concentrations of Hg(II) ions. (b) Photographic images of color of MPA–PDCA-modified gold nanoparticles (13 nM) in presence of different concentration of Hg (II) ion, (1) 3 ppm, (2) 6 ppm, (3) 10 ppm, (4) 50 ppm.

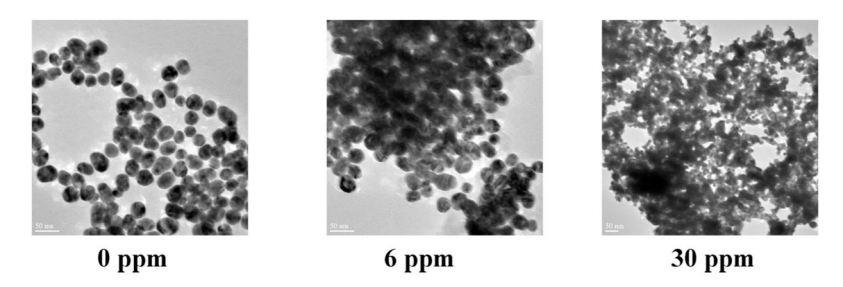


Figure 4.TEM images of MPA–PDCA-modified gold nanoparticle solution in the presence and in the absence of Hg(II) ions.

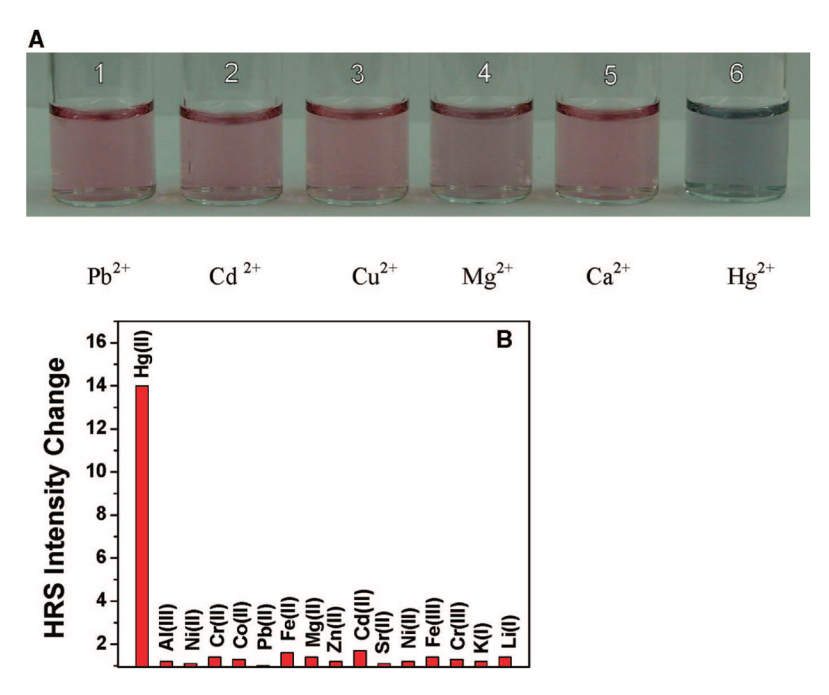


Figure 5.(a) Photographic images of color of MPA–HCys–PDCA-modified gold nanoparticles in presence of different metal ions with 40 ppm concentration. (b) HRS intensity change upon the addition of 40 ppm different metal ions on gold nanoparticle–MPA–HCys–PDCA solution (5 nM)